

# Comparison of Cloud Chemistry and Aerosol Parcel Model Simulations

*Mary Barth, Sonia Kreidenweis, and Rynda Hudman*

## 1. Introduction

The goal of Case 5, the cloud chemistry case, was to bring together cloud chemistry and aerosol scientists to discuss the representation of chemical constituents and aerosols as they are affected by cloud processes. Three parts of this case were addressed. The first, a box model simulation, assessed numerical approximation solver techniques of the gas-aqueous chemical system without aerosols. In addition, the effect of cloud chemistry on the gas-phase species was discussed. The second part, which was a parcel model simulation of aqueous-phase sulfur chemistry, was used to examine the predicted pH of the cloud drops and to contrast the results of models describing monodisperse aerosol particles and cloud drops with those describing polydisperse aerosol particles and cloud drops. The third part addressed the need to compare model results with observations. Simulations of stratocumulus observed in the Gulf of Maine during the NARE 1993 field campaign were conducted.

In all, 20 people participated in the Cloud Chemistry Case, where 5 of those 20 participated electronically. A sample of the results from each of these intercomparisons is presented.

## 2. Part 1: Idealized Cloud Chemistry Box Model Simulation

Over the past decade the effect of clouds on the oxidation, or cleaning capacity, of the atmosphere, in particular on tropospheric O<sub>3</sub>, has been debated. Lelieveld and Crutzen (1991) stated that clouds substantially affected O<sub>3</sub> concentrations, while Liang and Jacob (1997) and others have asserted that there is little or no effect of clouds on O<sub>3</sub>. To determine how well cloud chemistry simulations by different investigators agree, a cloud chemistry box model simulation was performed by seven different methods. This simulation primarily assessed the numerical solver technique used in the various models, but also pointed out some strengths and weaknesses in certain model code. To assess the influence of aqueous chemistry on gas-phase species, the end-points of a clear air simulation are compared to the cloudy air simulation.

### *CONDITIONS OF THE SIMULATIONS*

The simulation was based on case 10 from Lelieveld and Crutzen (1991). The scenario for this simulation was summer solstice at 45°N and 1.5 km altitude. The temperature was set to 285 K and constant noontime conditions were used for a 2 hour period. The chemical species and chemical reactions were the same as those listed in Lelieveld and Crutzen (1991) except that the reaction rate constants, equilibria constants, and accommodation coefficients were updated. These conditions can be found on the Cloud Modeling Workshop web site ([http://trwx.sws.uiuc.edu/wmoworkshop/Case5/Cloud\\_Chemistry.html](http://trwx.sws.uiuc.edu/wmoworkshop/Case5/Cloud_Chemistry.html)).

## NUMERICAL SOLUTION METHODS EMPLOYED BY THE PARTICIPANTS

Gas and aqueous chemistry is simulated in models using some form of this first-order, first degree, homogeneous, ordinary differential equation:

$$\frac{dC}{dt} = P - LC \quad (1)$$

where  $C$  is concentration,  $P$  is the chemical production of  $C$ , and  $L$  is the first-order loss term of  $C$ . Sets of gas and aqueous chemical reactions are stiff, meaning those whose species lifetimes vary by many orders of magnitude, thus only certain numerical solver methods are useful in solving them (Jacobson 1999). Table 1 provides information on the numerical solver of the seven models that participated in this case.

**Table 1.** Part 1 participants and features of their models.

<i>Participant</i>	<i>Solver Type</i>	Time Step	Gas-Aqueous Transport	Aqueous-Phase Dissociation	<i>Ref</i> <sup>a</sup>
<b>Barth</b>	Gear code	Variable, ≤ 4 min.	Diffusion limited	Forward-reverse reactions	
<b>Barth</b>	Gauss-Seidel Euler Backward Iterative	4 min.	Diffusion limited and equilibrium	Family equilibria	<b>B</b>
<b>Jacobson</b>	SMVGEAR	Variable, < 15 min	Diffusion limited	Family equilibria	<b>J</b>
<b>Kim</b>	VODE	≤ 1s	Diffusion limited	Family equilibria	
<b>Liang</b>	Newton-Raphson Iterative Method	5 min	Diffusion limited and equilibrium	Family equilibria	<b>LJ</b>
<b>Monod</b>	FACSIMILE	≤ 1s	Diffusion limited	Forward-reverse reactions	<b>CS</b>
<b>Sillman</b>	Euler Backward Iterative	5 min	Equilibrium	Family equilibria	<b>S</b>

<sup>a</sup>Definitions of references are **B** = Barth et al. (2001), **J** = Jacobson (1998), **LJ** = Liang and Jacobson (1999), **CS** = Curtis and Sweetenham (1987), **S** = Sillman (1991).

### *Gear Solver*

Four models (*Barth, Jacobson, Kim, Monod*) used some form of the Gear code. The Gear solver is a very accurate, predictor-corrector method of solving stiff systems. Time steps can vary based on the stiffness of the equations. If concentration is changing quickly, for example, the solver lowers the time step to get more accurate concentration values. The disadvantage of the original Gear method is that it is necessary to solve large-matrices of partial derivatives, hence limiting

its use in larger scale models. Two versions (*Barth, Jacobson*) have modifications that increase the speed of calculation.

### ***Euler-Backward Iterative***

The Euler backward iterative (EBI) method (*Barth, Sillman*), which is a stable, implicit method, solves Equation 1 as

$$C^{n+1,i+1} = \frac{C^n + P^{n+1,i} \Delta t}{1 + L^{n+1,i} \Delta t} \quad (2)$$

where  $n$  is the current time step,  $n+1$  is the next time step,  $\Delta t$  is the time step, and  $i$  represents the number of iterations. This scheme solves and updates equation 2 converging towards an answer for either a fixed number of iterations or, as in *Barth-EBI*, a threshold convergence criterion.

### ***Newton-Raphson Iterative***

The Newton Raphson method uses derivatives to converge upon a species concentration at a future time step. Equation 1 is solved as (*Liang and Jacobson, 1999*),

$$C^{i+1} - C^i = \frac{\Delta t(P - L) + C^0 - C^i}{I - \Delta t J} \quad (3a)$$

$$J = \frac{\delta(P - L)}{\delta C} \quad (3b)$$

where  $I$  denotes a unit matrix. The superscripts 0,  $i$ ,  $i+1$  denote the beginning of a time step, the  $i$ -th iteration and the  $(i+1)$ -th iteration, respectively.

### ***Other Methodology Considerations***

Besides the chemistry solver, the representation of transport across the gas-aqueous interface and of aqueous-phase dissociation may differ amongst models. *Barth-Gear, Jacobson, Kim*, and *Monod* determined mass transfer diffusion-limited transport in the gas-phase and across the drop interface. *Monod* also calculated aqueous-phase diffusion limitation. *Barth-EBI* and *Liang* treated most species to be in Henry's Law equilibrium and calculated diffusion-limited transport for a few short-lived species. *Sillman* established an equilibrium ratio for the gas and aqueous concentrations that was based on both the Henry's Law equilibrium and diffusion limitation in the gas-phase, across the interface, and in the drop. For those species that dissociate in the aqueous phase, *Barth-Gear* and *Monod* split these equilibria into forward and reverse reactions (and increased their reaction rates by several orders of magnitude), while others predict the total concentration in the aqueous phase and partition according to the equilibrium constant.

## METHODS

This case included two required simulations and six optional simulations (Table 2), all designed for midday conditions. Because all simulations were carried out within two hours of noontime, photodissociation rate coefficients were held constant for the entire run. Radiative effects by cloud drop scattering on photolysis frequencies in the air between cloud drops were not considered, but because refraction increases the pathlength inside the drops, in-cloud photolysis frequencies were increased by a factor of 1.5 compared to the gas-phase photolysis. The ending time values were compared between models and also between simulations.

**Table 2.** *Required and optional simulations performed for the intercomparison.*

<i>Required Simulations</i>	<i>Total Time</i>	<i>Time in cloud</i>
Cloudy Run	2 hours	11:30–12:30
Clear Air Run	2 hours	None
<i>Optional Simulations</i>	<i>Total Time</i>	<i>Time in cloud</i>
Intermittent cloud	2.8 hours	One hour (see text)
Expanded Mechanism	2 hours	11:30–12:30
Varying pH	2 hours	11:30–12:30
SO <sub>2</sub> chemistry	2 hours	11:30–12:30
Volatile Organic Compound chemistry	2 hours	11:30–12:30
Aerosols	2 hours	None

The first optional simulation simulated a 2.8-hour integration with one-hour of intermittent cloud. Thirty minutes of clear air was followed by 10 minutes of cloudy, non-cloudy intervals until a total of one-hour of cloudy air was reached. Clear air was included for the remainder of the run. The second optional simulation was to run the required simulation with an expanded mechanism, one that included more than the 58 reactions specified in the required simulation. Other optional simulations were varying pH, including volatile organic compound (VOC) chemistry, including SO<sub>2</sub> chemistry, and including aerosols.

## RESULTS

### *Required Simulations*

The first required base simulation introduced a cloud from 11:30 a.m. to 12:30 p.m.. We computed the average and standard deviation of the end points (Table 3) of all principle gas species. For the clear-sky-only simulation, the different models agreed well (<1% variation).

For the cloudy simulation, disagreement between simulations for the end points was greater, but still less than 7%. O<sub>3</sub> concentrations predicted by the models agreed well (Figure 1). Species, e.g. CH<sub>2</sub>O and HCOOH (Figure 2) showed less agreement between model solutions.

**Table 3.** Concentrations at the end of the required simulations' integration and the percent difference between the clear and cloudy simulations.

Species	Clear (molec cm <sup>-3</sup> )	Cloudy (molec cm <sup>-3</sup> )	Percent Difference (%)
O <sub>3</sub>	8.606(±0.004) x 10 <sup>11</sup>	8.453(±0.005) x 10 <sup>11</sup>	-1.78(±0.07)
H <sub>2</sub> O <sub>2</sub>	3.120(±0.014) x 10 <sup>10</sup>	3.431(±0.040) x 10 <sup>10</sup>	9.95(±1.26)
CH <sub>2</sub> O	9.195(±0.026) x 10 <sup>9</sup>	6.642(±0.368) x 10 <sup>9</sup>	-27.77(±1.44)
HCOOH	0.000	5.455(±0.664) x 10 <sup>8</sup>	∞
CH <sub>3</sub> OOH	6.730(±0.033) x 10 <sup>9</sup>	5.086(±0.082) x 10 <sup>9</sup>	-24.43(±1.39)
HO <sub>2</sub>	5.743(±0.013) x 10 <sup>8</sup>	5.698(±0.172) x 10 <sup>8</sup>	-0.79(±0.22)
CH <sub>3</sub> OO	2.930(±0.022) x 10 <sup>8</sup>	2.794(±0.091) x 10 <sup>8</sup>	-4.64(±0.98)
OH	1.266(±0.005) x 10 <sup>7</sup>	1.302(±0.047) x 10 <sup>7</sup>	2.81(±0.48)
NO	5.073(±0.009) x 10 <sup>8</sup>	5.496(±0.297) x 10 <sup>8</sup>	8.34(±1.19)
NO <sub>2</sub>	1.060(±0.003) x 10 <sup>9</sup>	1.127(±0.055) x 10 <sup>9</sup>	6.33(±1.01)
N <sub>2</sub> O <sub>5</sub>	1.450(±0.327) x 10 <sup>4</sup>	1.810(±0.527) x 10 <sup>4</sup>	24.89(±2.05)
NO <sub>3</sub>	7.876(±0.069) x 10 <sup>4</sup>	8.573(±0.658) x 10 <sup>4</sup>	8.85(±0.90)
HNO <sub>3</sub>	3.513(±0.003) x 10 <sup>9</sup>	3.363(±0.105) x 10 <sup>9</sup>	-4.25(±2.70)

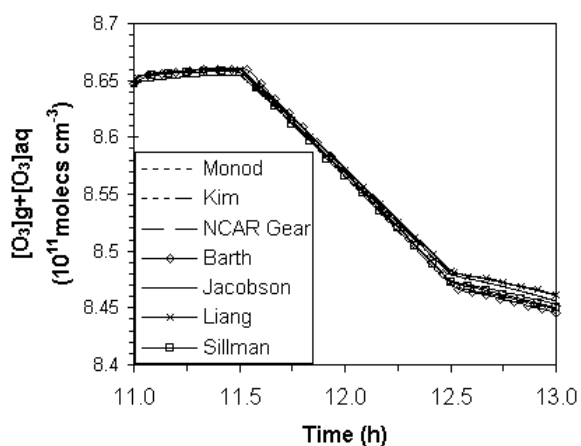


**Figure 1.** Total ozone concentration during the cloudy simulation.

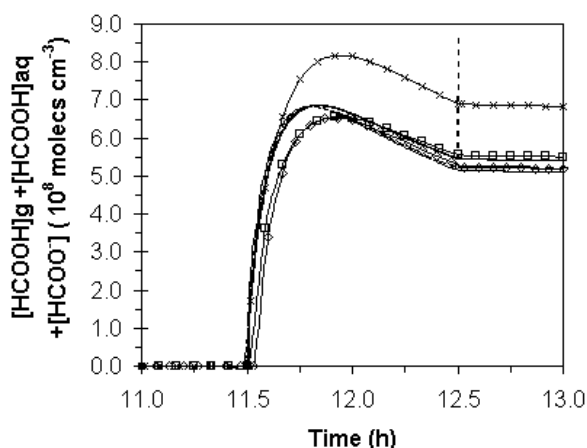


**Figure 2.** Total formic acid concentration during the cloudy simulation.

The results from *Liang*, who used the Newton-Raphson method to solve the set of gas and aqueous chemical reactions, were sometimes different than the results from the other simulations. At this point it is not obvious that the Newton-Raphson technique is causing the difference in model results from the other models, or if other factors in the model setup have caused the difference.

These other factors include the time step used by each participant, the method used for transferring a species between gas and aqueous phases, and the treatment of the aqueous-phase dissociation reactions. These factors appear to give a little more variability to the final concentration of species, but do not create significant differences in results.

### *Effect of Cloud Chemistry on Gas-Phase Species*

By comparing the endpoints of the clear sky only and the cloudy simulations, we can assess the influence of aqueous chemistry on tropospheric chemistry. Results listed in Table 3 indicate that O<sub>3</sub> is depleted by 1-2%. Formaldehyde (CH<sub>2</sub>O (g)) decreases ~30% after cloud exposure.

### *Optional Simulations*

Results from the optional simulations indicate that there is very little effect on O<sub>3</sub> concentrations at the end of the simulation period compared to the required simulation (Table 4). Formaldehyde concentrations were affected much more, especially for the simulation that included VOCs, the intermittent cloud simulation, and the variable pH simulation.

**Table 4.** *Percent difference between the optional simulation and the required cloudy simulation for the end of each simulation.*

Optional Simulation	O <sub>3</sub>	CH <sub>2</sub> O
Variable pH	0.9%	10.7%
Intermittent Cloud	-0.1%	-10.2%
Expanded Mechanism 1	0.0%	-1.5%
Expanded Mechanism 2	0.0%	-4.9%
VOCs Included	-0.1%	14.2%
SO <sub>2</sub> Included	0.1%	-5.1%

## *SUMMARY OF PART 1*

We found that the idealized box model simulations are a valuable way to diagnose differences between model descriptions of gas-aqueous chemistry. Plots of other species for both the required and optional simulations may be found on the web at <http://acd.ucar.edu/~barthm/Part1results.html>. Now that some basic parameters have been tested, further scenarios, using box models, should be explored. One suggestion is to configure the box model to a parcel model study, similar to what was done for Part 2 of the Cloud Chemistry Case. Other additions include scenarios with varying pH, sulfur chemistry, and constant NO<sub>x</sub> conditions. A passive, soluble tracer should be included in all future case studies.

## **3. Part 2: Aerosol Parcel Model**

The role of clouds in processing gases and aerosols has been a focus of interest for a number of years. Both bulk-type chemistry and size-resolved, or bin, chemistry have been incorporated into models on a variety of spatial scales. Recently, simulations have also sought to examine the modification of input aerosol spectra by addition of nonvolatile mass by aqueous-phase chemical

processes. Particle growth by this mechanism is important for aerosol direct and indirect forcing estimates. The Part 2 case study was designed to examine differences in S(IV) to S(VI) conversion and pH predictions between bulk and bin chemistry models, and also to examine how different models add S(VI) to the input aerosol size distribution.

### *CONDITIONS OF THE SIMULATIONS*

The simulation was for sulfur oxidation with an initial aerosol composition (ammonium bisulfate), mass concentration ( $2 \mu\text{g SO}_4^{2-} \text{ m}^{-3}$ ,  $0.375 \mu\text{g NH}_4^+ \text{ m}^{-3}$ ), and lognormal size distribution specified. A simple chemical mechanism that converted S(IV) to S(VI) via  $\text{O}_3$  and  $\text{H}_2\text{O}_2$  oxidation was provided. Participants were asked to run this mechanism assuming bulk chemistry and assuming size-resolved chemistry. Optional simulations, wherein the bulk and size-resolved models were run with any mechanism, were invited, but results from the optional runs will not be reported here.

The parcel to be simulated was lifted adiabatically with an updraft velocity of  $50 \text{ cm s}^{-1}$ . Cloud base temperature and pressure were 284.2 K and 939 mb, respectively, and the models were to be run for 1200 m (40 min) above cloud base. The initial gas-phase species concentrations were as follows:  $\text{SO}_2$ , 200 pptv;  $\text{NH}_3$ , 100 pptv;  $\text{H}_2\text{O}_2$ , 500 pptv;  $\text{HNO}_3$ , 100 pptv,  $\text{O}_3$ , 50 ppbv;  $\text{CO}_2$ , 360 ppmv. Based on the initial aerosol composition and gas-phase species concentrations oxidation of S(IV) by  $\text{H}_2\text{O}_2$  was expected to be the dominant mechanism. The full problem statement can be found at the Cloud Modeling Workshop web site.

### *RESULTS: BULK CHEMISTRY CASE*

Table 5 lists the participants in the bulk chemistry case and some salient model features. All of the models include gas- and interfacial-mass transfer resistances; one model (*Walcek*) also

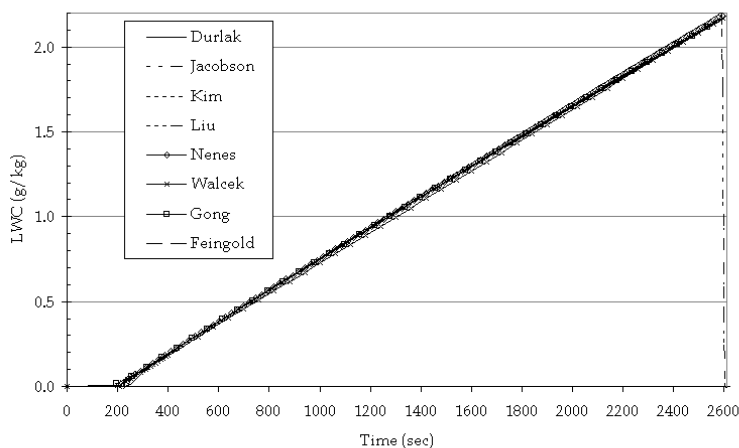
*Table 5. Part 2, bulk chemistry: participants and features of their models.*

<i>Participant</i>	<i>Gas phase and Interfacial resistance</i>	<i>Aqueous-phase resist.</i>	<i>Standard pH?</i>	<i>Other notes</i>
Durlak	Both		Excludes $\text{CO}_2$	
Feingold	Both			
Gong I	Both			10 $\mu\text{m}$ fixed
Gong II	Both			Variable Dd
Jacobson	Both		Adds $\text{HO}_2^-$	Activity coeffs
Kim	Both			
Liu	Both			
Nenes	Both			
Walcek	Both	X		mass transfer rate= chemical reaction rate in drop

includes aqueous-phase mass transfer resistances. In general, the species included in the computation of pH are similar in all models, except for one (*Durlak*), which neglects CO<sub>2</sub> and its dissolution products.

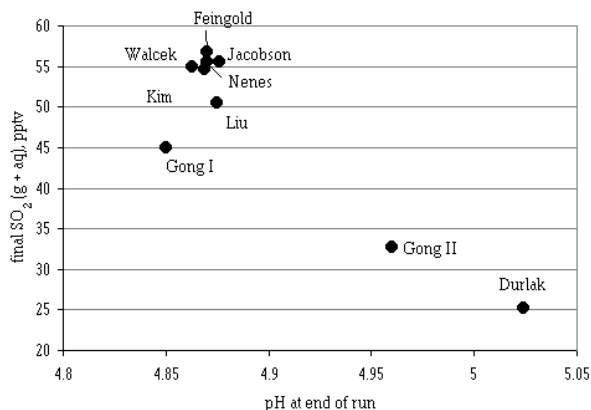
Although participants were asked to assume a 10 μm droplet size for purposes of computation of mass transfer rates for the bulk cases, different assumptions were sometimes employed because the models were set up to be more sophisticated than this. Some models (e.g., *Gong II*) allow drop size to grow as the liquid water content (LWC) of the cloud increases. *Gong II* also employs a parameterization of droplet activation wherein not all the initial aerosol is automatically incorporated into cloud.

Figure 3 shows the LWC in the parcel computed by each participant. Agreement among the various models is quite good, with some minor differences most likely arising from assumptions of the values of thermodynamic variables. *Jacobson* includes a drop to low relative humidity at the end of the simulation in order to “dry out” the aerosol for reporting final size distributions in the bin chemistry case.



**Figure 3.** LWC as a function of time for Part 2, bulk chemistry case.

Figures 4 and 5 show results for the conversion predicted by each model. In Figure 4, the final total [SO<sub>2</sub>] is plotted against the predicted pH. Six of the models cluster closely with [SO<sub>2</sub>] between 50 and 57 pptv, and pH between 4.86 and 4.88. From this result, the effect of varying treatments of mass transfer resistance does not seem to be very large for this case. The *Gong I* model predicts a similar pH but somewhat more conversion of SO<sub>2</sub>. The *Gong II* model has a somewhat higher pH, which may be due to the effect of not incorporating all the initial aerosol into cloud. The *Durlak* model predicts the largest conversion and highest pH among the models.



**Figure 4.** Final total SO<sub>2</sub> (SO<sub>2</sub>(g) + S(IV)) as a function of final pH.

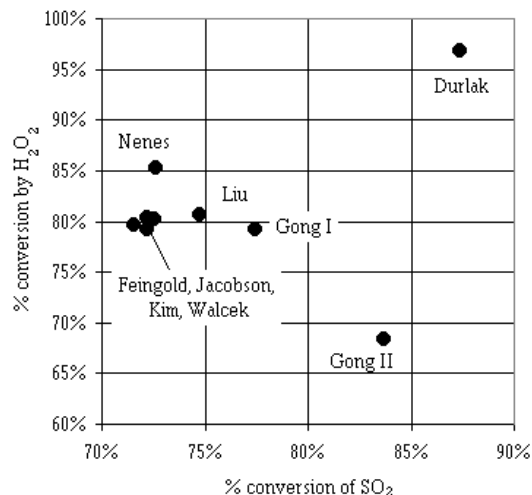


**Figure 5.** Percentage of total conversion of initial SO<sub>2</sub> that proceeds via reaction with H<sub>2</sub>O<sub>2</sub> (ordinate) vs. total % conversion of SO<sub>2</sub> for various models (abscissa).

In Figure 5, the percentage conversion of SO<sub>2</sub> is shown on the x-axis, and is seen to be between 72% and 78% for 7 of the models. Of the converted SO<sub>2</sub>, the percent via the H<sub>2</sub>O<sub>2</sub> oxidation pathway is shown on the y-axis. Five of the models predict about 80% due to this pathway. The *Gong II* model predicts more overall conversion with less conversion via H<sub>2</sub>O<sub>2</sub>, suggesting that the higher pH raised the significance of the O<sub>3</sub> reaction pathway for this simulation.

#### RESULTS: BIN CHEMISTRY CASE

Table 6 lists the participants in the bin chemistry case and some salient model features. All of the models included gas- and interfacial-mass transfer resistances. The number of aerosol bins varied widely. An estimate of the number concentration of aerosol particles activated to drops (in

**Table 6.** Part 2, bin chemistry: participants and features of their simulations.

<i>Participant</i>	<i>Gas phase and interfacial resistance</i>	<i># aerosol bins</i>	<i># drops (max), cm<sup>-3</sup></i>
Durlak	Both	64	420
Feingold	Both	20	268
Gong	Both	20	267
Jacobson	Both	50	145
Liu	Both	30	358
Nenes	Both	30	365

number  $\text{cm}^{-3}$ , at cloud top density) is also provided. These numbers are not exact as the definition of “drop” can be rather arbitrary; generally, the number concentrations of drops with diameters larger than  $1 \mu\text{m}$  were reported. The initial aerosol number concentration (at cloud base density) was  $566 \text{ cm}^{-3}$ .

The final pH values in the bin chemistry runs (Figure 6) are not very different from those in the bulk chemistry runs. There are two clusters of predicted final pH: a cluster of three models that predict  $\text{pH} \sim 4.82$ , and the remainder which predict  $\text{pH} \sim 5.1$ . Interestingly, the latter group contains the models with the larger number of aerosol bins. As shown in Figure 6, the pH variations do not correspond to systematic variations in the extent of conversion of S(IV). In fact, all of the bin chemistry models predict that 85-90% of the initial  $\text{SO}_2$  is oxidized (Figure 7). This extent of conversion is higher than most of the bulk model predictions, and indeed each bin model predicts more conversion than its bulk counterpart. This result is in agreement with the findings from earlier comparison studies that have been published in the literature (e.g., Hegg and Larson, 1990; Roelofs, 1993).

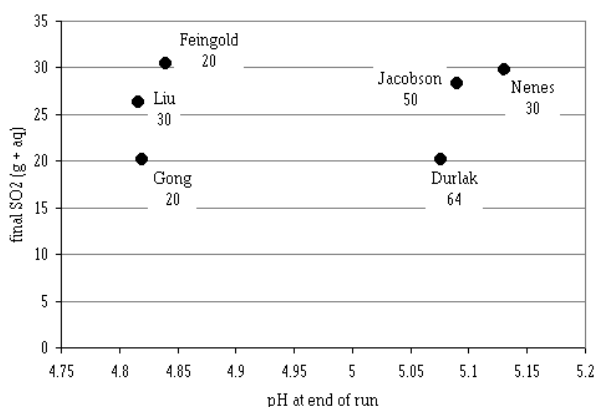


**Figure 6.** Final total  $\text{SO}_2$  ( $\text{SO}_2(\text{g}) + \text{S}(\text{IV})$ ) as a function of final (overall) pH, in the bin chemistry case. The number of bins used in each model is shown below the participant’s name.

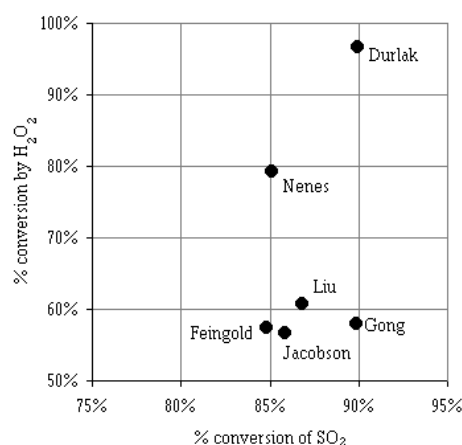


**Figure 7.** Percentage of total conversion of initial  $\text{SO}_2$  that proceeds via reaction with  $\text{H}_2\text{O}_2$  (ordinate) vs. total % conversion of  $\text{SO}_2$  for various models (abscissa), for the bin chemistry case.

Figure 7 presents a plot similar to that shown for the bulk cases, where both the extent of conversion of initial  $\text{SO}_2$  and the role of  $\text{H}_2\text{O}_2$  in oxidation are examined. For all of the models except *Durlak*, the role of  $\text{O}_3$  has been enhanced in the bin chemistry case relative to that in the bulk chemistry cases.

The addition of sulfate mass onto the input aerosol size distribution is examined by plotting the final S(VI) mass dry aerosol size distribution (Figure 8). We note that the size distributions should properly be shown as histograms, but that we have approximated them by plotting the

value of the distribution function at the bin midpoint diameter. As a result, some of the distributions appear broader, but their main features can be distinguished. All of the models predict significant growth via mass addition onto relatively small particles, with the final dry sizes of the grown particles between about 0.1 and 0.3  $\mu\text{m}$ . Three of the models (*Durlak*, *Feingold*, and *Liu*) predict the main “spike” in approximately the same location ( $\sim 0.17 \mu\text{m}$ ) while the remaining three (*Gong*, *Jacobson* and *Nenes*) predict the grown size to be slightly larger. This sorting does not correspond to differences in predicted conversion or final pH, but may be related to the different number concentrations of particles activated to droplets. Specifically, models that activate fewer droplets are expected to grow the aerosol inside those drops to larger sizes, since the S(VI) that is produced in-cloud is distributed among fewer particles. Further, when fewer particles are activated, the separation of small and larger particles is emphasized because the initial mean sizes of the activated particles that are grown by the sulfur chemistry are larger than in the cases activating more particles.

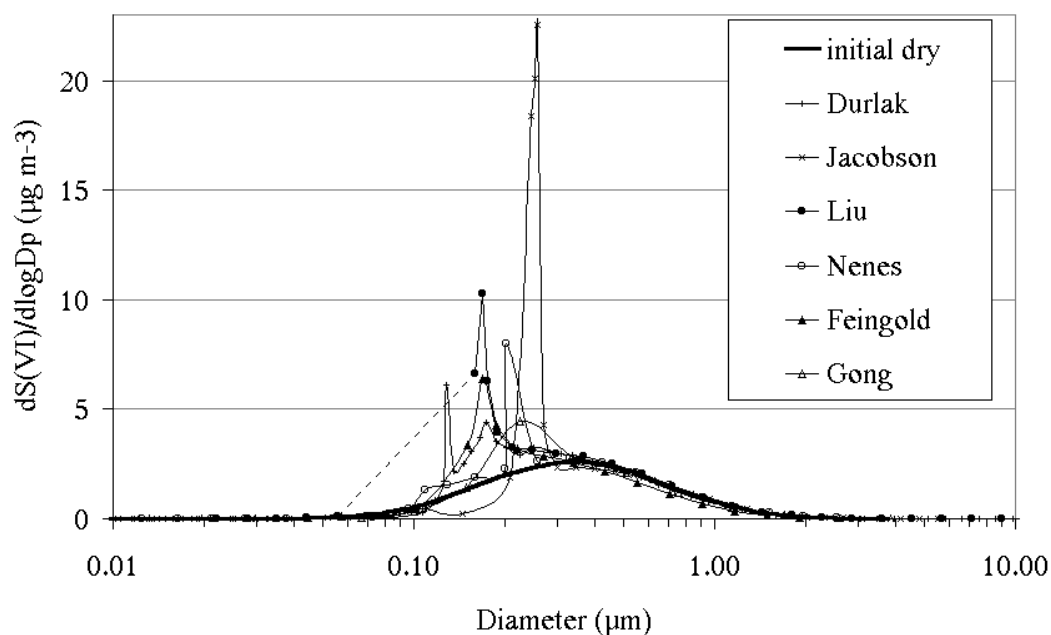


**Figure 8.** Final dry aerosol size distributions of S(VI) mass. Solid black line indicates input aerosol distribution.

## SUMMARY OF PART 2

We found that the parcel model simulations were an effective tool for learning about different modeling approaches to aerosol/cloud interaction problems. Surprisingly, the group expended significant effort early in the process on reconciling different estimates of LWC in the adiabatic parcels, finally agreeing to input a single common profile for the purposes of this workshop. This very basic aspect of models should be given careful attention in future intercomparison studies, as variations in LWC can significantly affect predictions of chemical conversion.

Our studies confirmed that bin chemistry models oxidize more S(IV) than do bulk models. This is most likely an effect of the pH variations across the drop spectrum, since we showed that the role of O<sub>3</sub> in S(VI) production is enhanced in the bin models. The models do not all agree on how the added S(VI) mass modifies the (dry) aerosol size distribution. Model resolution of the aerosol and drop spectra probably plays some role, but our results suggest that differences in activation schemes have probably the largest impact on the predictions. The differences in modified aerosol spectra found among models would probably translate into noticeable differences in estimates of the resulting direct and indirect aerosol forcing.

The participants agreed that the size-resolved simulations could be fruitfully extended to learn more about model sensitivities. The potential importance of the aerosol activation scheme in both the bulk and bin chemistry simulations suggests that further exploration of activation schemes be a future focus. Examination of predicted drop spectra and size-dependent pH should be pursued in upcoming studies. It would also be of interest to compare model predictions with observations; a case close to the adiabatic parcel approach used here is that of an orographic cloud. Data sets obtained for ACE-2 orographic clouds may be useful for such comparisons. Other suggestions for elements in future workshops included: link the simulations in Part 1 and Part 2; simulate external mixtures of aerosol composition; add mineral particles; and examine the effects of organic species and variable solubility. A long-term goal of this portion of the workshop should be examination of aerosol-cloud interaction parameterizations used in models simulating such interactions on a variety of spatial scales.

#### **4. Part 3: Marine Stratocumulus Simulation**

The purpose of Part 3 is to compare model results with observations. The case is taken from the 1993 summer intensive measurement campaign of the North Atlantic Regional Experiment (NARE). The measurements for this case were conducted over the Bay of Fundy and Gulf of Maine within a 100 km radius of Yarmouth, Nova Scotia, Canada (near 44°N and 66°W) from 15 August to 8 September. This case focused on the September 4–7 time period after a cold front passed across the Gulf of Maine and the area came under the influence of high pressure. During this period, surface winds were light and air near the surface originated over the ocean east of Florida. Air at 500 mb came from over the continent. Low stratus developed during the afternoon of September 5 and by late in the day covered the sampling area. The stratus formed below 800 m as a result of the cooling of warmer and moister air from the south as it was advected over the cooler waters in the Bay of Fundy and Gulf of Maine. These conditions persisted throughout Sept. 5-7. Measurements of gas and aqueous-phase chemical species, aerosol physical characteristics, and cloud physical parameters were obtained from six flights on board the AES Twin Otter.

This case was suitable for both regional-scale and cloud-scale simulations, for which initialization conditions of the cloud-scale simulations are given on the Cloud Modeling Workshop web site. Three groups expressed interest in this case, but only one group performed the simulation. The Meteorological Service of Canada (participants: Nina Ivanis (MSC), Richard Leaitch (MSC), and Hong Lin (MSC)) used NARCM to simulate sulfate aerosols on the regional scale.

Comparison of the results from the NARCM model to observations showed that the boundary layer structure was not modeled properly, which might be related to poorly described subgrid processes in the meteorology model. There was disagreement between the measured species concentrations and the simulated values because the models did not represent the marine boundary layer (MBL) properly. High concentrations of species that were observed above the MBL (about 300 m) were simulated to be at the surface. This discrepancy is currently being investigated.

We decided that this case is actually quite difficult to simulate. The stable boundary layer is decoupled from the cloudy layer and to maintain cloud, water vapor must be advected into the region.

We recommend that for a model-observation intercomparison, that an easier case be used. For example, orographic clouds would provide a measurement scenario for parcel models to represent. Experiments during Great Dun Fell, ACE-2, and ACE-Asia may provide the needed meteorological and chemical observations for an intercomparison. The convectively-driven (or cloud-topped radiatively cooled) marine boundary layer, such as those found off the coast of California or during ASTEX near the Azores, could be another candidate for a model-observation intercomparison.

## **5. Recommendations for the Cloud Chemistry Case**

Since the Cloud Modeling Workshop in August 2000, many investigators have resubmitted results for Parts 1 and 2. These updated results are shown here. Subsequent discussions of these results and other cloud chemistry investigations will be pursued at Spring AGU 2001. We were pleased at the success of the electronic submission and recommend its use in the future. We feel that electronic submission increased the number of participants in the Cloud Chemistry Case. We would speculate that technology advances during the next 4 years, would allow computer-projected viewing of results, on-site calculations, and web-based conferencing with participants off-site. We urge the organizers of the next workshop to implement the infrastructure to allow for these technological advances.

## **6. Acknowledgments**

We would like to thank all the participants of the Cloud Chemistry Case for their time spent performing model runs and helping with the analysis of results: Susan Durlak (NCAR), Graham Feingold (NOAA/ETL), Wanmin Gong (MSC), Nina Ivanis (MSC), Mark Jacobson (Stanford U.), Cheol-Hee Kim (CSU), Richard Leitch (MSC), Jinyou Liang (CARB), Hong Lin (MSC), Xiaohong Liu (U. Mich.), Anne Monod (LCE), Athanasios Nenes (CalTech), Irena Pavnova (U. McGill), Nicole Shantz (MSC), Sanford Sillman (U. Mich.), and Chris Walcek (SUNY-Albany).

## 6. References

- Barth, M.C., A.L. Stuart, W. C. Skamarock (2001) Numerical simulation of the July 10 Stratospheric-Tropospheric Experiment: Radiation, Aerosols, and Ozone/Deep Convection storm: Redistribution of soluble tracers, submitted to *J. Geophys. Res.*
- Curtis, A.R. and W. P. Sweetenham, (1987) AERE Report R-12805, UK Atomic Energy Research Establishment, 1987.
- Hegg, D. A., and T. V. Larson, (1990) The effects of microphysical parameterization on model predictions of sulfate production in clouds, *Tellus*, **B42**, 272-284.
- Jacobson, M.Z. (1999) *Fundamentals of Atmospheric Modeling*, Cambridge University Press, Cambridge, UK.
- Jacobson, M.Z. (1998) SMVGEAR II, Improvement of SMVGEAR II on vector and scalar machines through absolute error tolerance control, *Atmos. Environ.*, **32**, 791-796.
- Leaitch, W.R. et al (1996) Physical and chemical observations in marine stratus during the 1993 North Atlantic Regional Experiment: factors controlling cloud droplet number concentrations, *J. Geophys. Res.*, **101**, 29,123-29,135.
- Lelieveld, J. and P.J. Crutzen (1991) The role of clouds in tropospheric photochemistry, *J. Atmos. Chem.*, **12**, 229-267.
- Liang, J. and D. J. Jacob (1997) Effect of aqueous-phase cloud chemistry on tropospheric ozone, *J. Geophys. Res.*, **102**, 5993-6002.
- Liang, J. and M.Z. Jacobson (1999) A study of sulfur dioxide oxidation pathways over a range of liquid water contents, pH values, and temperatures, *J. Geophys. Res.*, **104**, 13,749-13,769.
- Roelofs, G. J. H., (1993) A cloud chemistry sensitivity study and comparison of explicit and bulk cloud model performance, *Atmos. Environ.*, **27A**, 2255-2264.
- Sillman, S., (1991) A numerical solution to the equations of tropospheric chemistry based on an analysis of sources and sinks of odd hydrogen, *J. Geophys. Res.*, **96**, 20,735-20,744.